energies

MDPI

Article

Modeling of the Chemical Looping Combustion of Hard Coal and Biomass Using Ilmenite as the Oxygen Carrier

Anna Zylka [1,*], Jaroslaw Krzywanski [1], Tomasz Czakiert [2], Kamil Idziak [2], Marcin Sosnowski [1], Marcio L. de Souza-Santos [3], Karol Sztekler [4] and Wojciech Nowak [4]

1 Faculty of Science and Technology, Jan Dlugosz University in Czestochowa, 42-200 Czestochowa, Poland; j.krzywanski@ujd.edu.pl (J.K.); m.sosnowski@ujd.edu.pl (M.S.)
2 Department of Advanced Energy Technologies, Czestochowa University of Technology, 42-201 Czestochowa, Poland; tczakiert@is.pcz.czest.pl (T.C.); k.idziak@is.pcz.pl (K.I.)
3 Department of Energy, School of Mechanical Engineering, University of Campinas, Campinas, SP 13083-970, Brazil; dss@csfmb.com
4 Faculty of Energy and Fuels, AGH University of Science and Technology, 30-059 Cracow, Poland; sztekler@agh.edu.pl (K.S.); wnowak@agh.edu.pl (W.N.)
* Correspondence: a.zylka@ujd.edu.pl

Received: 15 September 2020; Accepted: 12 October 2020; Published: 15 October 2020

Abstract: This paper presents a 1.5D model of a fluidized bed chemical looping combustion (CLC) built with the use of a comprehensive simulator of fluidized and moving bed equipment (CeSFaMB) simulator. The model is capable of calculating the effect of gas velocity in the fuel reactor on the hydrodynamics of the fluidized bed and the kinetics of the CLC process. Mass of solids in re actors, solid circulating rates, particle residence time, and the number of particle cycles in the air and fuel reactor are considered within the study. Moreover, the presented model calculates essential emissions such as CO_2, SO_X, NO_X, and O_2. The model was successfully validated on experimental tests that were carried out on the Fluidized-Bed Chemical-Looping-Combustion of Solid-Fuels unit located at the Institute of Advanced Energy Technologies, Czestochowa University of Technology, Poland. The model's validation showed that the maximum relative errors between simulations and experiment results do not exceed 10%. The CeSFaMB model is an optimum compromise among simulation accuracy, computational resources, and processing time.

Keywords: chemical looping combustion; CeSFaMB; ilmenite; oxygen carrier; hard coal; biomass

1. Introduction

Global climate change caused by the greenhouse effect is the main reason to look for new solutions for burning solid fuels. One of the most promising combustion methods with inherent CO2 separation is chemical looping combustion (CLC) technology, which uses oxygen carriers (OCs) in the fuel combustion process. This technology requires two separate fluidized bed reactors: air reactor (AR) and fuel reactor (FR) with circulating and bubbling fluidized bed, respectively. In the AR the OCs are oxidized. In contrast, the OCs are reduced in the FR's reaction chamber, as shown in Figure 1 [1,2].

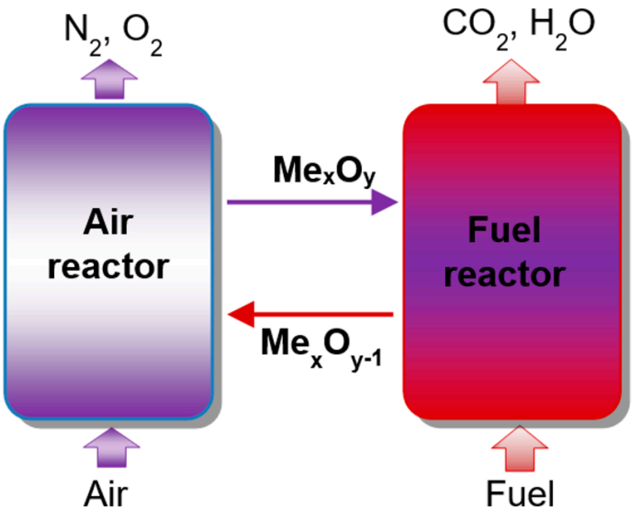

Figure 1. The scheme of the chemical looping combustion (CLC) process.

OCs are usually metals or metal oxides characterized with specific properties such as high mechanical resistance, high oxygen transfer capacity, adequate specific heat capacity, and low production costs. However, their most crucial advantage is their neutral impact on the environment [3–6].

In this work, ilmenite is selected as an OC. This natural mineral is characterized by good thermal properties and excellent mechanical resistance but reveals a tendency to agglomerate at high temperatures. In addition, ilmenite has a relatively low oxygen transfer capacity compared to, e.g., copper oxide [7–9].

This paper is a continuation and extension of previous work [1]. The novelty of the developed model is the use of a different oxygen carrier (ilmenite) and two different fuels: hard coal and biomass.

The two fuels used in this study differ mainly in their origin. Hard coal is a fossil and is considered a non-renewable energy source. Biomass grows above the ground, and during the photosynthesis process, it absorbs as much CO_2 as it releases during the combustion processes. Therefore, biomass is considered a carbon-neutral energy source and is much more environmentally friendly than hard coal. Thus, biomass combustion is one of the ways that helps to achieve greenhouse gas emission reduction targets. Biomass differs from lignite in many characteristics: carbon, sulfur, oxygen, ash, and volatile matter content, and the heating value [10,11]. Moreover, coal has a higher calorific value than biomass. In addition, there are also some differences in the content of the other components. Biofuels usually have a high sodium and potassium content, leading to lower ash softening points. This may cause operational problems during the combustion process, e.g., defluidization as the effect of the bed sintering, superheater fouling, and high-temperature corrosion [10–15].

2. Materials and Methods

The work aimed to develop a CLC model for biomass and coal as fuel and ilmenite as OC. The result is a 1.5-dimensional model where the simulation tool was the comprehensive simulator of fluidized and moving bed equipment (CeSFaMB) simulator.

In addition, the presented model permits a comparison of the simulation results of two different fuels (biomass and coal) combustion using the same OC. The comparison applies to both hydrodynamics of the fluidized bed as well as CO_2, SO_X, and NO_X emissions.

The ilmenite, imported from the Titania AS ilmenite ore mine on Norway's southwest coast, was used as an OC in experimental and model studies. This natural mineral consists primarily of $FeTiO_3$ ($FeO{\cdot}TiO_2$), but the active phase is an iron oxide that belongs to the iG-CLC process, meaning that it releases oxygen in the FR only after direct contact with the fuel [16–19].

The following properties of ilmenite were considered in the study:

1. density: 3879 kg/m^3,
2. Sauter mean diameter of particles: 161 μm,
3. sphericity: 0.65.

A microscopic photograph of the OC is given in Figure 2, and its particle size distribution is shown in Figure 3.

Figure 2. The microscopic photograph of ilmenite.

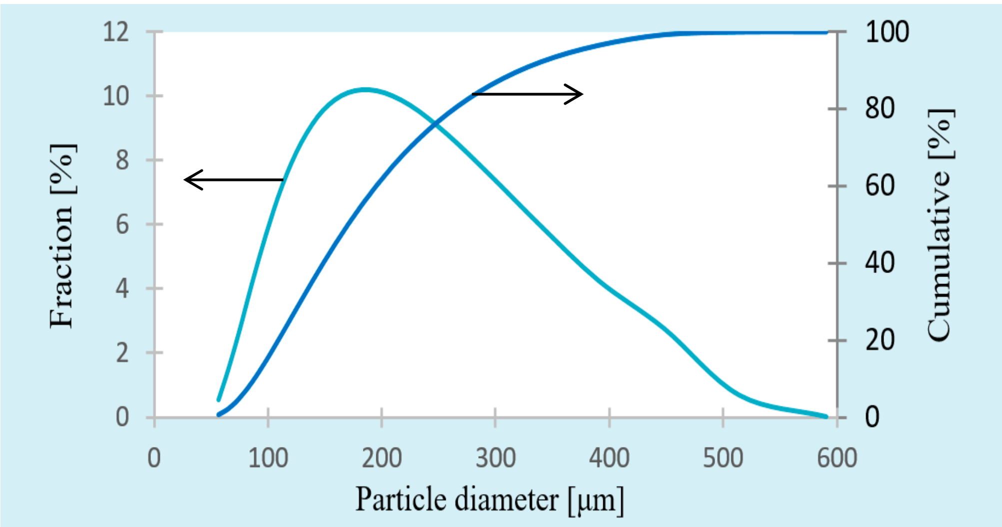

Figure 3. The particle size distribution of ilmenite.

Wood chips (biomass) and hard coal from the Polish coal mine "Sobieski" were used as solid fuels. Microscopic photographs of biomass and coal are shown in Figure 4, and particle size distribution of the fuels are given in Figures 5 and 6, respectively.

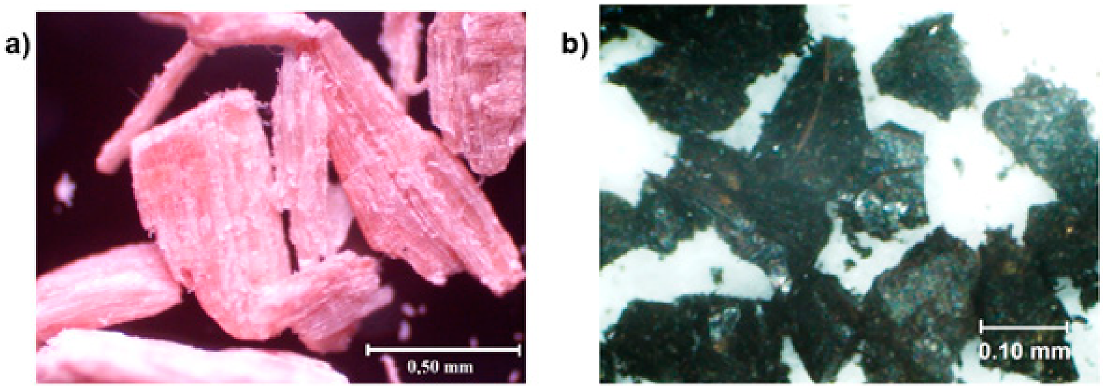

Figure 4. The microscopic photograph of fuel: (**a**) biomass (**b**) hard coal.

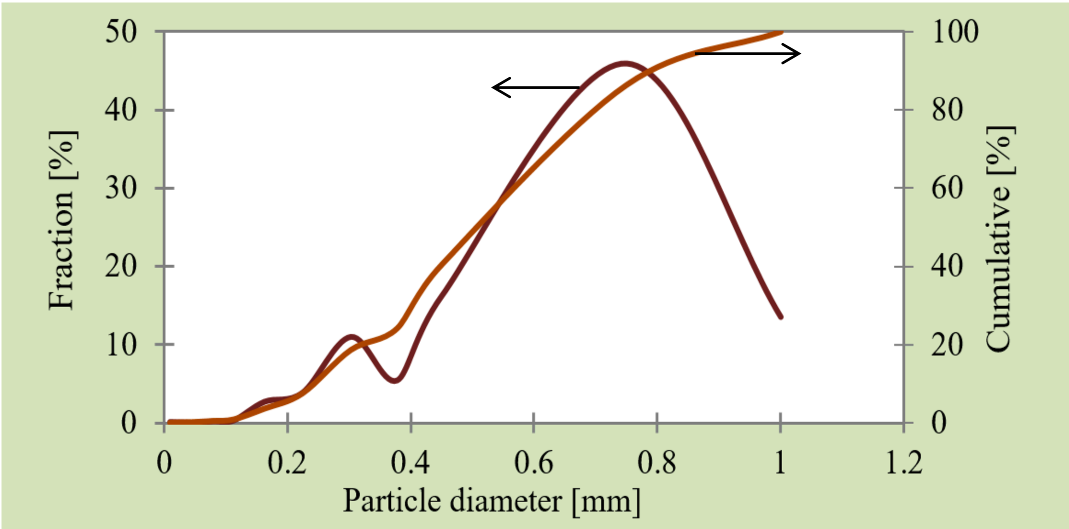

Figure 5. The particle size distribution of biomass.

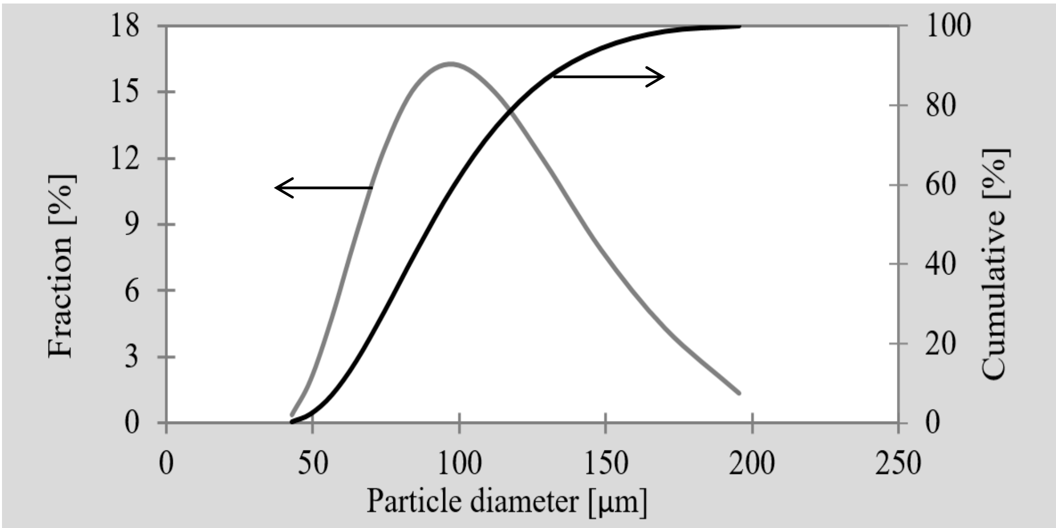

Figure 6. The particle size distribution of hard coal.

The detailed analysis of hard coal and biomass composition is presented in Table 1.

Table 1. Proximate and ultimate analysis of hard coal and biomass.

Proximate Analysis/wt. %	Hard Coal	Biomass
Net calorific value [kJ/kg]	23,429	17,253
Moisture, % (wet)	13.30	6.20
Ash, % (wet)	8.20	1.40
Volatile, % (wet)	29.49	77.00
Fixed carbon	49.01	15.40
Ultimate Analysis/wt. %		
Carbon, % (wet)	61.90	47.70
Hydrogen, % (wet)	3.66	5.47
Nitrogen, % (wet)	0.99	0.27
Total sulfur, % (wet)	1.39	0.11
Oxygen, %	10.56	38.95

The FB-CLC-SF Unit

Experimental studies were carried out on the Fluidized Bed—Chemical Looping Combustion of Solid Fuel (FB-CLC-SF) unit. The research unit's schematic diagram is given in Figure 7. This unit is located at the Institute of Advanced Energy Technologies, Czestochowa University of Technology, Poland.

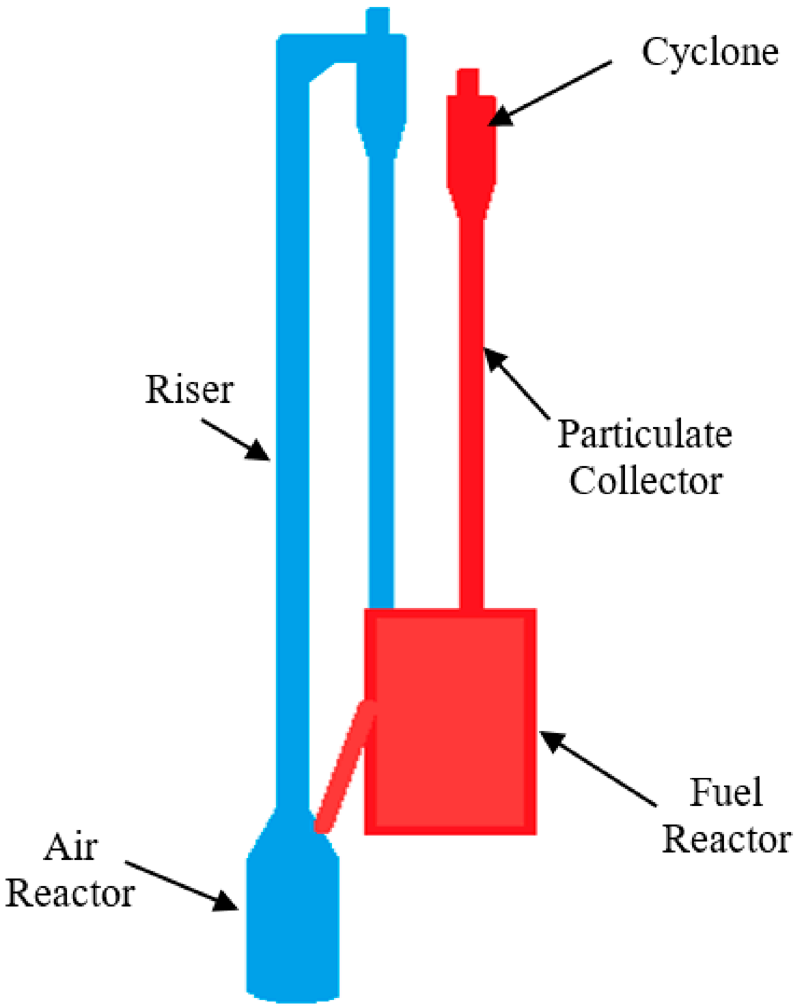

Figure 7. The scheme of the Fluidized Bed—Chemical Looping Combustion of Solid Fuel (FB-CLC-SF) unit.

The comprehensive CeSFaMB simulator was applied in the study, as the software is dedicated to fluidized bed analysis. This simulator provides information at each point throughout the unit. The results obtained are dimensional simulations and consider differential mass and energy balances for all phases throughout the bed and the freeboard [20–23].

CeSFaMB was successfully used as a modeling tool in many scientific papers for various objects such as furnaces, boilers, dryers, and gasifiers [23–25], including applications of the CLC processes [1,3,26–28].

Validation of the developed model concerning hydrodynamics, including the mass of solids in reactors, solids circulating rate, particle residence time, and the number of particle cycles in the reactors, was successfully performed in [1,3]. The maxi mum relative error between experimental and numerical results does not exceed 10%. The developed model was also used to determine emissions, i.e., CO_2, SO_X, (SO_2 + SO_3), and NO_X (NO + NO_2 + N_2O).

The CeSFaMB simulator allows for the performance of numerical simulations only after defining the boundary and initial conditions. These primary operational data necessary to perform the simulation process are listed in Table 2.

Table 2. The operational conditions of the FB-CLC-SF unit.

Operational Parameters	Value	
	Test with Biomass	Test with Hard Coal
Average bed temperature in AR, [K]	1078	1152
Average bed temperature in FR, [K]	1079	1156
Absolute pressure below the gas distributor in AR, [Pa]	103,935	104,148
Absolute pressure below the gas distributor in FR, [Pa]	104,659	105,360
Total mass of solids in the AR, [kg]	1.61	1.42
Total mass of solids in the FR, [kg]	2.91	2.36
Gas mass flow rate in AR, [$\times 600^{-1}$ kg s^{-1}]	4.21	4.21
Gas mass flow rate in FR, [$\times 600^{-1}$ kg s^{-1}]	6.52	6.52
Fuel mass flow rate, [kg s^{-1}]	8×10^{-6}	8×10^{-6}

The models prepared by CeSFaMB are classified into the 1.5D models. This is because, despite the overall 1D (axial) approach, the model also computes some essential variables based on the 2D approach. These include the point-by-point circulation rates of particles in the bed. Then, the radial variations are integrated to provide the average in the axial direction. The basic equations are fundamental differential mass and energy balances using the classic Eulerian approach. The CeSFaMB simulator also uses auxiliary semi-empirical relations to evaluate bed dynamic, heat, and mass transfer parameters. The Eulerian approach is also applied to evaluate the circulation rates of particles inside the bed. However, when it comes to relations to compute reactions within solid particles, the model uses the Lagrangian approach.

The results obtained with the CeSFaMB software are in good agreement with the experimental ones. The maximum relative error does not exceed 10%. The calculations carried out by the CeSFaMB simulator are not time-consuming compared to other methods, including the CFD approach. A detailed description of the CeSFaMB simulator can also be found elsewhere [1]

Since the active phase in ilmenite is iron oxide, the CLC model presented in this work takes into account the set of the following chemical equations [1,3]:

$$2Fe + O_2 = 2FeO \quad (1)$$

$$3Fe + O_2 = Fe_3O_4 \quad (2)$$

$$4Fe + 3O_2 = 2Fe_2O_3 \quad (3)$$

$$Fe_2O_3 + 3H_2 = 2Fe + 3H_2O \quad (4)$$

$$Fe_3O_4 + 4H_2 = 3Fe + 4H_2O \quad (5)$$

$$FeO + H_2 = Fe + H_2O \quad (6)$$

$$Fe_2O_3 + 3CO = 2Fe + 3CO_2 \quad (7)$$

$$Fe_3O_4 + 4CO = 3Fe + 4CO_2 \quad (8)$$

$$FeO + CO = Fe + CO_2 \quad (9)$$

$$FeO + CO_2 = FeCO_3 \quad (10)$$

$$4Fe_2O_3 + 3CH_4 = 8Fe + 3CO_2 + 6H_2O \quad (11)$$

$$Fe_2O_3 + 3H_2 = 2Fe + 3H_2O \quad (12)$$

$$Fe_2O_3 + 3CO = 2Fe + 3CO_2 \quad (13)$$

The kinetics of chemical reactions, as well as the dynamics of the fluidized bed, have been presented in the literature [29].

3. Results and Discussion

3.1. CLC Model Validation

The first attempts to validate the CLC model for ilmenite using the CeSFaMB simulator were presented in other studies [3,27]. This paper shows numerical simulations with the latest version of the CeSFaMB 4th generation for biomass and coal CLC combustion with ilmenite oxygen carrier. The CLC model's validation includes such parameters as the average temperature in the reactors, pressure drop in the fluidized bed, void fractions, gas mass flow rate, superficial gas velocity, and primary emissions: CO_2, O_2, NO_X, SO_X.

3.1.1. The Average Temperature in the Reactors

The AR's average temperature in both experiments with hard coal and wood chips was similar and amounted to 1152 K and 1156 K, respectively. In the FR, the average temperature in both experimental tests was similar and equal to 1078 K and 1079 K, respectively.

The comparison of the experimental results with numerical simulations for the average temperature in reactors is depicted in Figure 8. The maximum relative error for this parameter is equal to 1.39%.

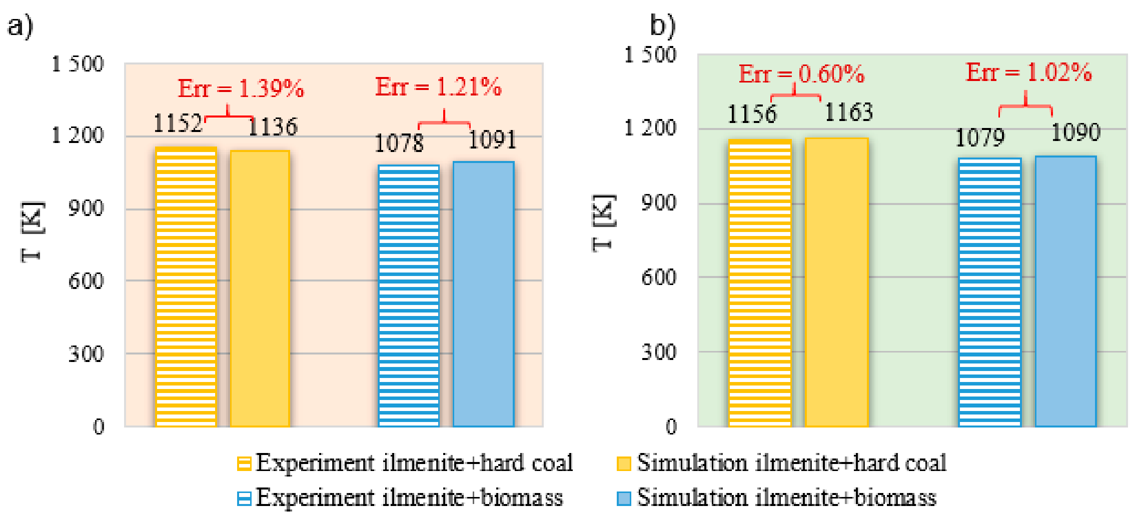

Figure 8. The average temperature in the reactors: (**a**) air reactor (AR) (**b**) fuel reactor (FR).

3.1.2. Pressure Losses in the Fluidized Bed

The pressure decreases with the height of the fluidized bed. This phenomenon is referred to as a pressure drop in the fluidized bed; the greater the height of the dense fluidized bed, the greater the pressure drop in the bed [30].

The highest dense fluidized bed in the FR, i.e., 0.39 m, was observed during ilmenite experiments with biomass. Therefore, in this case, the pressure drop was the highest and amounted to 2822 Pa. The second highest dense fluidized bed in the FR, equal to 0.38 m, was noticed for ilmenite with hard coal CLC combustion. The pressure drop was 2755 Pa, in this case.

The lowest pressure drops were recorded in the AR for the ilmenite-hard coal test. The 0.30 m height of the dense fluidized bed corresponded to a pressure drop of 1879 Pa. Similar to previous observations, higher pressure drops in the AR were obtained for ilmenite with biomass test. In this case, the height of the dense fluidized bed was 0.32 m and, the pressure drop was 2303 Pa.

The maximum relative error between the experiment results and the numerical simulation results for the bed pressure drop was about 3%, as shown in Figure 9.

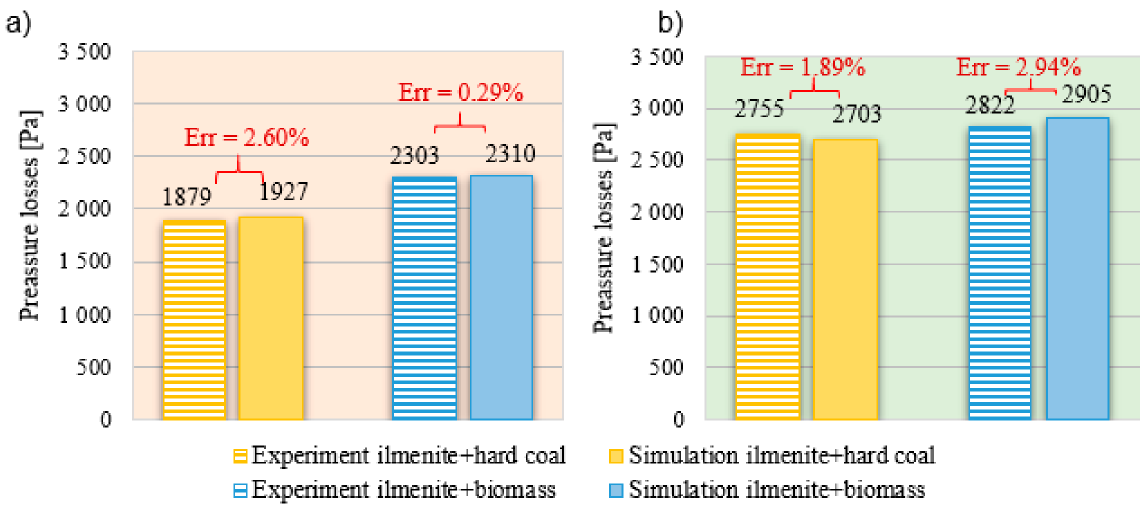

Figure 9. Pressure drop in the fluidized bed (**a**) AR (**b**) FR.

3.1.3. Void Fractions

A fluidized bed consists of dense and lean regions located in the lower and the upper parts of the reaction chamber, respectively. A high concentration of solid material characterizes the dense part of the fluidized bed. Moreover, as mentioned before, the most significant pressure drop occurs in this part of the reactor.

The experimental value for void fractions (vf) is determined in the following steps:

1: Pressure sensors are located along with the reactor chamber every few centimeters. The pressure measurements along the reactor's length determine the lean and dense part of the fluidized bed. Then, using the classic formula for the pressure loss:

$$\Delta p = q_{fb} \cdot g \cdot h$$

where Δp = pressure difference between sensors [Pa]; q_{fb} = bulk density of fluidized bed at a specific height of the reactor [kg/m^3]; g = 9.81 m/s^2 acceleration of gravity; h = height between sensors [m].

2: From the formula above, the bulk density is determined as:

$$q_{fb} = \frac{\Delta p}{g \cdot h}$$

3: Then, knowing the particle true density (q_P) the formula below is used to determine void fractions:

$$vf = 1 - \frac{q_{fb}}{q_P}$$

Figures 10 and 11 show the comparison between experiment and simulation results for void fractions of the fluidized bed in the AR and FR.

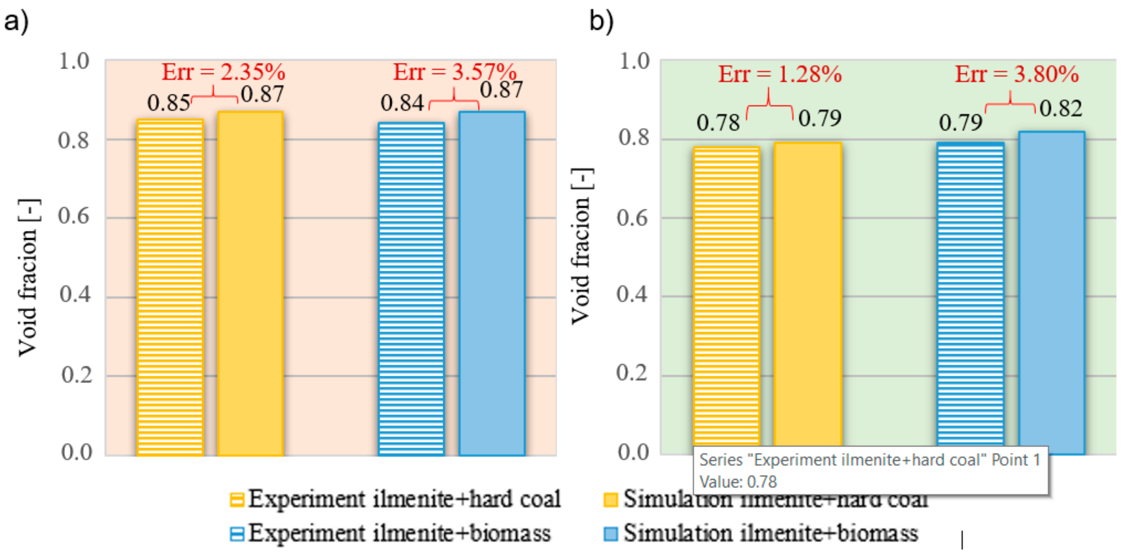

Figure 10. Experiment and simulation results for the dense region: (**a**) AR (**b**) FR.

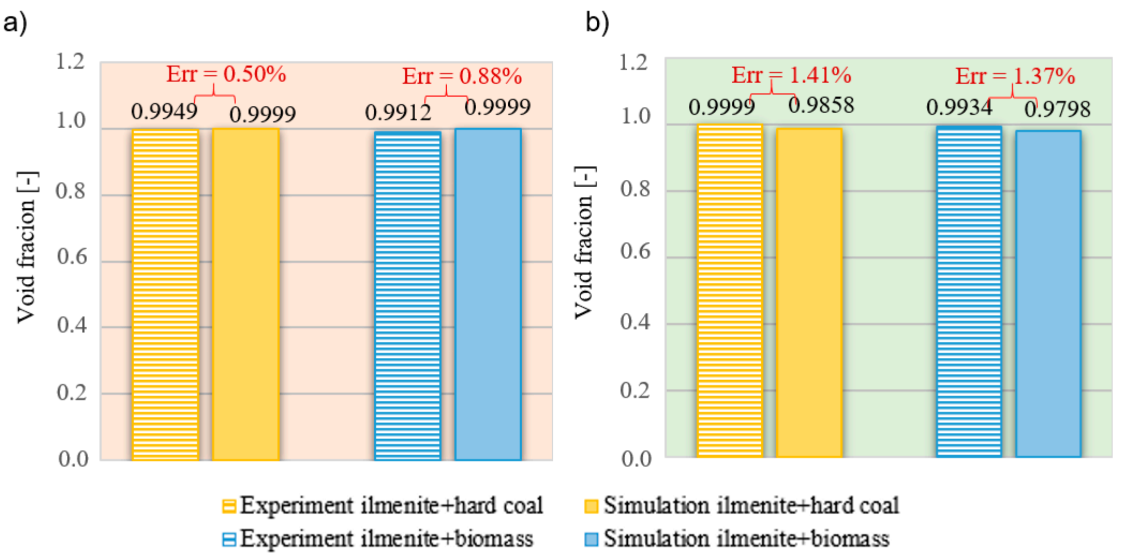

Figure 11. Experiment and simulation results for the lean region:(**a**) AR (**b**) FR.

As indicated in the above Figure 10 and Figure 11, the maximum relative errors between simulation and experimental results are 0.88% for the dense region and 1.41% for the lean part of the fluidized bed, respectively.

3.1.4. Gas Mass Flow Rate

Figure 12 shows the comparison between measured and calculated results for the gas mass flow rates in both AR and FR. The CO_2 was fed to the FR while the AR was supplied by air.

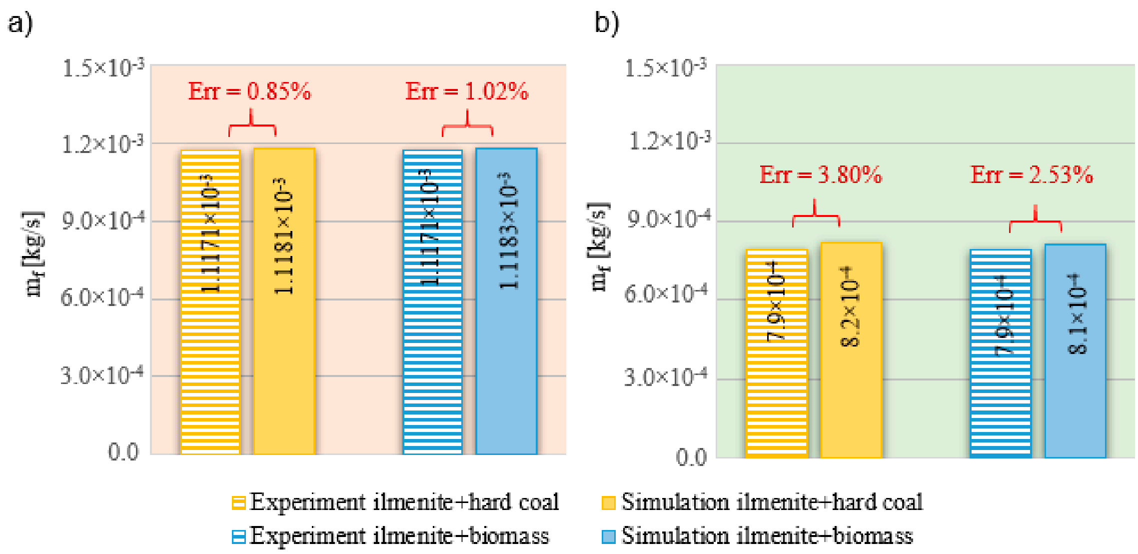

Figure 12. Experiment and simulation results for gas mass flow rate: (**a**) AR (**b**) FR.

The above comparison showed that the maximum relative error for the gas mass flow rate is 3.8% in the FR and 1.02% in the AR.

3.1.5. Superficial Gas Velocity in the Bed

The comparison between measured and calculated results for superficial gas velocity in the AR and FR is shown in Figure 13.

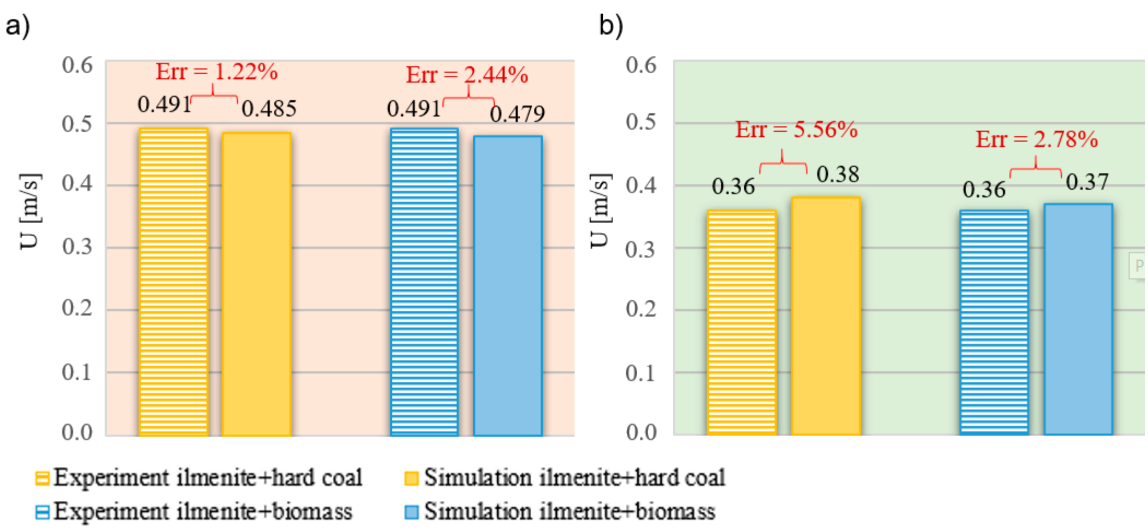

Figure 13. Superficial gas velocity in the bed (**a**) AR (**b**) FR.

The maximum relative errors for superficial gas velocity are lower than 5.56% for the FR and 2.44% for the AR.

3.1.6. Emissions

The emissions for hard coal and biomass are shown in Table 3.

Table 3. Experiment and simulation results concerning emissions in the AR and FR.

Fuel	Emission	Experiment	Simulation	Err [%]
Fuel Reactor				
Biomass	CO_2 [%]	98.27	97.80	0.49
Hard coal		98.09	97.40	0.70
Biomass	O_2 [ppm]	0.00	0.00	0.00
Hard coal		0.00	0.00	0.00
Biomass	SO_X [ppm]	9.24	10.15	9.85
Hard coal		85.55	78.60	8.12
Biomass	NO_X [ppm]	124.93	113.10	9.47
Hard coal		56.22	61.40	9.21
Air Reactor				
Biomass	O_2 [%]	20.27	20.19	0.39
Hard coal		18.09	19.47	7.87

As can be seen, there is no oxygen in emissions. Since the ilmenite is an OC that belongs to the iG-CLC OCs group, oxygen is released in direct contact with the fuel and is consumed immediately. Therefore, no oxygen was recorded in the flue gas.

Model validation taking into account essential emissions for hard coal and biomass as fuels showed that the maximum relative error between the experiment and simulation results does not exceed 10%.

3.2. A CLC Model

The developed CLC model also allows taking into account the effects of the superficial gas velocity in the FR on fluidization hydrodynamics and emissions during CLC combustion in the FB-CLC-SF unit.

3.2.1. Solid Circulating Rate

The effect of superficial gas velocity in a FR on a solid circulating rate is shown in Figure 14.

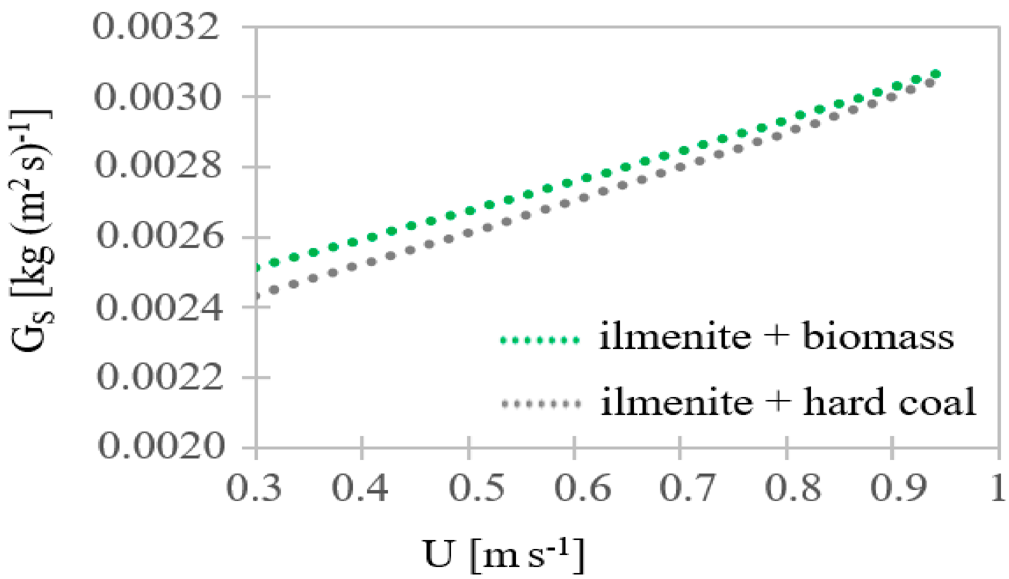

Figure 14. The solid circulating rates of the ilmenite versus superficial gas velocity in the FR.

The increase in superficial gas velocity in the combustion chamber causes the increase of the solids circulating rate in both cases. The following equations describe these correlations:

$$G_{S\ (ilmenite+biomass)} = 0.0023e^{0.31U} \tag{14}$$

$$G_{S\ (ilmenite+hard\ coal)} = 0.0022e^{0.35U} \tag{15}$$

3.2.2. Mass of the Solid Fraction in Reactors

Figure 15 shows the total mass of solids in the reactors versus superficial gas velocity in the FR.

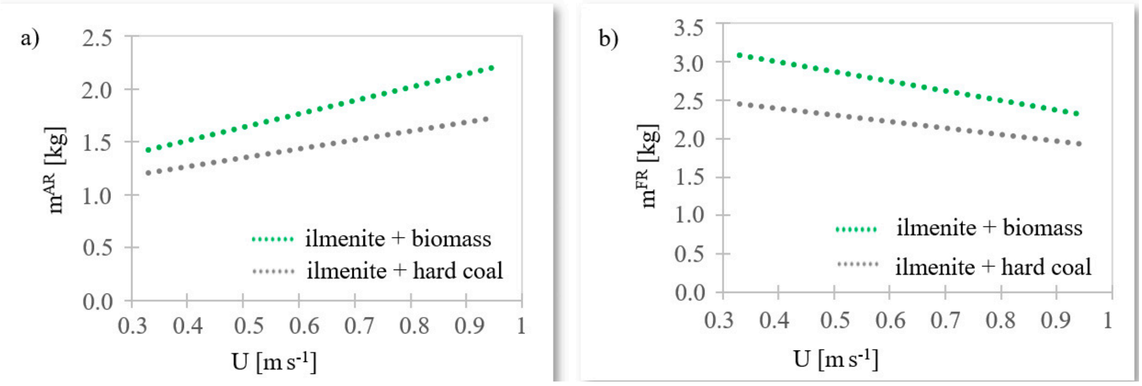

Figure 15. The total mass of solids in the fuel reactor (**a**) and air reactor (**b**) versus the superficial gas velocity in the FR.

The increase in the mass of material in the AR and decrease in the FR results from an increase in the superficial gas velocity in FR and is described by Equations (16)–(19):

$$m^{AR}_{(ilmenite+biomass)} = 1.26U + 1.01 \tag{16}$$

$$m^{AR}_{(ilmenite+hard\ coal)} = 0.84U + 0.93 \tag{17}$$

$$m^{FR}_{(ilmenite+biomass)} = -1.26U + 3.50 \tag{18}$$

$$m^{FR}_{(ilmenite+hard\ coal)} = -0.84U + 2.72 \tag{19}$$

3.2.3. Particles' Residence Time

The superficial gas velocity in both reactors affects many of the analyzed parameters, including the mass of material in the reactors, which in turn affects the residence time of the particles in the reactors. Figure 16 shows the particles' residence time in the reactors versus superficial gas velocity in the FR.

The increase of superficial gas velocity in an FR causes an increase in the particles' residence time in the AR and a decrease in the particles' residence time in the FR. This behavior can be described by formulas Equations (20)–(23):

$$t^{AR}_{R\ (ilmenite+biomass)} = 719.05U^{0.20} \tag{20}$$

$$t^{AR}_{R\ (ilmenite+hard\ coal)} = 566.45U^{-0.10} \tag{21}$$

$$t^{FR}_{R\ (ilmenite+biomass)} = 753.74U^{0.48} \tag{22}$$

$$t^{FR}_{R\ (ilmenite+hard\ coal)} = 633.17U^{-0.46} \tag{23}$$

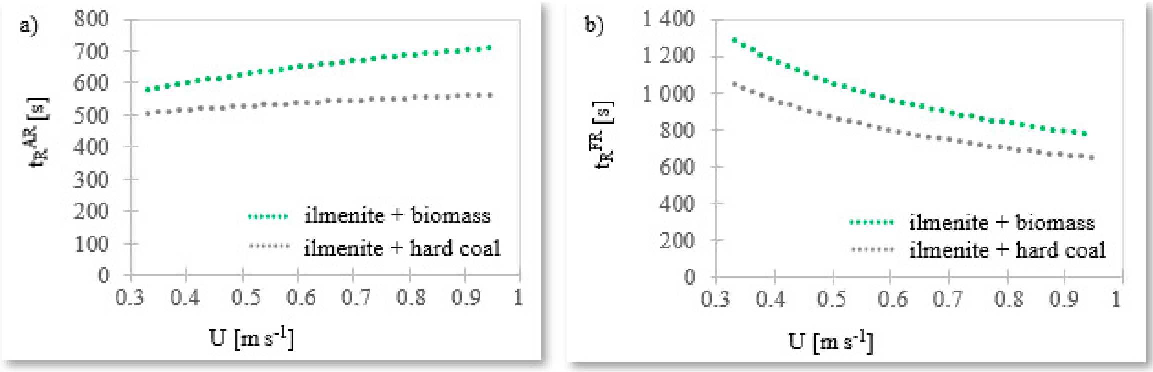

Figure 16. The particles' residence time in the reactors versus superficial gas velocity in the FR (**a**) AR; (**b**) FR.

3.2.4. The Number of Oxygen Carrier Cycles

The number of OC cycles indicates how many times the particle will flow through the reactor in one hour. The number of OC cycles in reactors versus superficial gas velocity in the FR is shown in Figure 17.

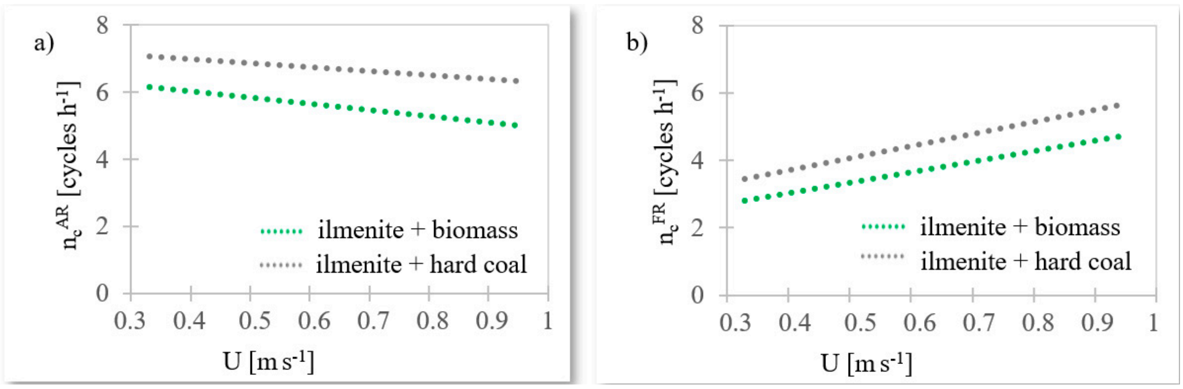

Figure 17. The number of ilmenite cycles in reactors versus superficial gas velocity in the FR (**a**) AR; (**b**) FR.

The decrease in the number of OC cycles in the AR and increase of OC cycles in the FR is resulting from an increase in the superficial gas velocity in FR, as described by Equations (24)–(27):

$$n^{AR}_{c(\text{ilmenite+biomass})} = -1.88U + 6.78 \quad (24)$$

$$n^{AR}_{c(\text{ilmenite+hard coal})} = -1.16U + 7.45 \quad (25)$$

$$n^{FR}_{c(\text{ilmenite+biomass})} = 3.12U + 1.78 \quad (26)$$

$$n^{FR}_{c(\text{ilmenite+hard coal})} = 3.61U + 2.25 \quad (27)$$

3.2.5. Emissions from the Fuel Reactor

The primary gas emissions versus the superficial gas velocity in the FR are shown in Figure 18. The effect of superficial gas velocity in FR on CO_2, SO_X, and NO_X emissions can be described by the following Equations (28)–(33):

$$CO^{dry}_{2\ (\text{ilmenite+biomass})} = 0.92\ln(U) + 98.47 \quad (28)$$

$$CO_{2\ (\text{ilmenite+hard coal})}^{\text{dry}} = 0.89\ln(U) + 98.73 \quad (29)$$

$$SO_{X\ (\text{ilmenite+biomass})}^{\text{dry}} = -0.58\ln(U) + 9.56 \quad (30)$$

$$SO_{X\ (\text{ilmenite+hard coal}}^{\text{dry}} = -3.38\ln(U) + 58.43 \quad (31)$$

$$NO_{X\ (\text{ilmenite+biomass})}^{\text{dry}} = -10.98\ln(U) + 102.7 \quad (32)$$

$$NO_{X\ (\text{ilmenite+hard coal})}^{\text{dry}} = -3.65\ln(U) + 75.18 \quad (33)$$

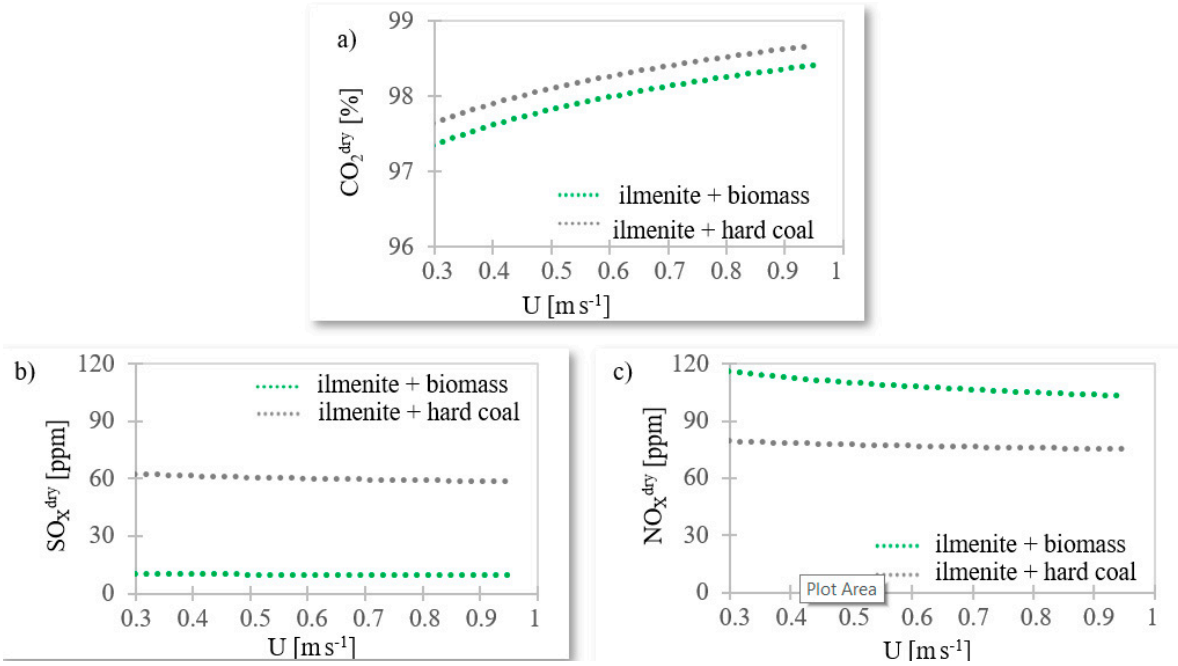

Figure 18. The emissions from hard coal and biomass combustion versus the superficial gas velocity in the FR: (**a**) CO_2, (**b**) SO_X, (**c**) NO_X.

The increase of superficial gas velocity in the FR causes a significant increase in CO_2 emissions, shown in Figure 18a. Since CO_2 constitutes the FR's fluidizing gas, it dilutes other flue gas components, leading to the decrease in SO_X and NO_X emissions, shown in Figure 18.

The high concentration of CO_2 in the exhaust gas (97–99%) confirms that the end product is practically pure CO_2 that can be stored. Thus, energy is saved for the capture of CO_2 from the flue gas, which proves the thermoeconomic benefits [31–35].

4. Conclusions

The CLC model developed and presented in this work concerns ilmenite as an OC and two different solid fuels, i.e., wood chips and hard coal. The model was successfully validated against measured data. The relative error calculated during the validation of the developed model does not exceed 10%.

The increase in superficial gas velocity leads to an increase in the number of OC cycles and the decrease in the mass of materials and residence time of the particles in the FR. Moreover, the increase in gas superficial velocity in the FR causes the increase of CO_2 emissions and a simultaneous decrease in NO_x and SO_x concentrations in the flue gas. The increase in CO_2 concentrations is because the fuel reactor is fluidized by CO_2, hence the dilution of the other flue gas components concentrations.

The obtained high concentration of CO_2 in the exhaust gas means that there is no need to clean the exhaust gas of CO_2, which is favorable from the thermoeconomic point of view.

Author Contributions: Conceptualization, A.Z., J.K. and T.C.; methodology, A.Z., K.I., M.S.; software, M.L.d.S.-S.; validation, A.Z., M.L.d.S.-S., and M.S.; formal analysis, W.N.; investigation, K.I. T.C., A.Z. and K.S.; resources, J.K., W.N. and K.S.; data curation, T.C., K.I.; writing—original draft preparation, A.Z.; writing—review and editing, J.K. and M.S.; visualization, K.I., K.S.; supervision, J.K., W.N.; project administration, T.C.; funding acquisition, J.K., T.C., W.N. All authors have read and agreed to the published version of the manuscript.

Funding: This research received no external funding.

Acknowledgments: This scientific work was funded from Norway Grants in the Polish-Norwegian Research Program, operated by the National Centre for Research and Development. Project: Innovative Idea for Com bustion of Solid Fuels via Chemical Looping Technology. Scientific work was performed within the project No. 2018/29/B/ST8/00442, supported by the Na tional Science Center (Narodowe Centrum Nauki). The support is gratefully acknowledged.

Conflicts of Interest: The authors declare no conflict of interest.

Nomenclature

CeSFaMB	Comprehensive Simulator of Fluidized and Moving Bed equipment
FB-CLC-SF	The Fluidized-Bed Chemical-Looping-Combustion of Solid-Fuels
CLC	Chemical Looping Combustion
AR	Air reactor
FR	Fuel reactor
OC	Oxygen carrier
iG-CLC	in-situ Gasification Chemical Looping Combustion
U	Superficial gas velocity [$m\ s^{-1}$]
m_f	Gas mass flow rate [$kg\ s^{-1}$]
G_S	Solid circulating rate [$kg\ (m^2\ s)^{-1}$]
n_c	Number of oxygen carrier cycles [cycles h^{-1}]
t_R	Particles residence time [s]
m	Mass of solid in reactors [kg]

References

1. Zylka, A.; Krzywanski, J.; Czakiert, T.; Idziak, K.; Sosnowski, M.; Grabowska, K.; Prauzner, T.; Nowak, W. The 4th Generation of CeSFaMB in numerical simulations for CuO-based oxygen carrier in CLC system. *Fuel* **2019**, *255*, 115776. [CrossRef]
2. Sosnowski, M.; Krzywanski, J.; Gnatowska, R. Polyhedral meshing as an innovative approach to computational domain discretization of a cyclone in a fluidized bed CLC unit. *E3S Web Conf.* **2017**, *14*, 01027. [CrossRef]
3. Zylka, A.; Krzywanski, J.; Czakiert, T.; Idziak, K.; Kulicki, K.; Jankowska, S.; Nowak, W. A 1.5 D model for the chemical looping combustion system with ilmenite. In Proceedings of the 8th European Combustion Meeting, Dubrovnik, Croatia, 18–21 April 2017; pp. 1785–1790.
4. Pröll, T.; Mayer, K.; Bolhàr-Nordenkampf, J.; Kolbitsch, P.; Mattisson, T.; Lyngfelt, A.; Hofbauer, H. Natural minerals as oxygen carriers for chemical looping combustion in a dual circulating fluidized bed system. *Energy Procedia* **2009**, *1*, 27–34. [CrossRef]
5. Adánez, J.; Cuadrat, A.; Abad, A.; Gayán, P.; de Diego, L.F.; García-Labiano, F. Ilmenite activation during consecutive redox cycles in chemical-looping combustion. *Energy Fuels* **2010**, *24*, 1402–1413. [CrossRef]
6. Cuadrat, A.; Abad, A.; Adánez, J.; de Diego, L.F.; García-Labiano, F.; Gayán, P. Behavior of ilmenite as oxygen carrier in chemical-looping combustion. *Fuel Process. Technol.* **2012**, *94*, 101–112. [CrossRef]
7. Idziak, K.; Czakiert, T.; Krzywanski, J.; Zylka, A.; Nowak, W. Emissions of NOx and SOx from fluidized-bed chemical-looping-combustion of solid-fuel (FB-CLC-SF) with ilmenite as an oxygen carrier. In Proceedings of the 8th European Combustion Meeting, Adria Section of the Combustion Institute, Dubrovnik, Croatia, 18–21 April 2017; pp. 1769–1774.
8. de Diego, L.F.; García-Labiano, F.; Adánez, J.; Gayán, P.; Abad, A.; Corbella, B.M.; María Palacios, J. Development of Cu-based oxygen carriers for chemical-looping combustion. *Fuel* **2004**, *83*, 1749–1757. [CrossRef]

9. Ksepko, E.; Klimontko, J.; Kwiecinska, A. Industrial wastewater treatment wastes used as oxygen carriers in energy generation processes. *J. Therm. Anal. Calorim.* **2019**, *138*, 4247–4260. [CrossRef]
10. Krzywański, J.; Rajczyk, R.; Nowak, W. Model research of gas emissions from lignite and biomass co-combustion in a large scale CFB boiler. *Chem. Process. Eng.* **2014**, *35*, 217–231. [CrossRef]
11. Krzywanski, J.; Rajczyk, R.; Bednarek, M.; Wesolowska, M.; Nowak, W. Gas emissions from a large scale circulating fluidized bed boilers burning lignite and biomass. *Fuel Process. Technol.* **2013**, *116*, 27–34. [CrossRef]
12. Abelha, P.; Gulyurtlu, I.; Crujeira, A.T.; Cabrita, I. Co-combustion of several biomass materials with bituminous coal in a circulating fluidized bed combustor. In Proceedings of the 9th International Conference on Circulating Fluidized Beds in Conjunction with the 4th International VGB Workshop Operating Experience with Fluidized Bed Firing Systems, Hamburg, Germany, 15–16 May 2008.
13. Werther, J. Potentials of biomass co-combustion in coal-fired boilers. In Proceedings of the 20th International Conference on Fluidized Bed Combustion, Xi'an, China, 18–21 May 2009; Yue, G., Zhang, H., Zhao, C., Luo, Z., Eds.; Springer: Berlin/Heidelberg, Germany, 2010; pp. 27–42.
14. Jenkins, B.M.; Baxter, L.L.; Miles, T.R.; Miles, T.R. Combustion properties of biomass. *Fuel Process. Technol.* **1998**, *54*, 17–46. [CrossRef]
15. Leckner, B. Co-combustion: A summary of technology. *Therm. Sci.* **2007**, *11*, 5–40. [CrossRef]
16. Adanez, J.; Abad, A.; Garcia-Labiano, F.; Gayan, P.; de Diego, L.F. Progress in chemical-looping combustion and reforming technologies. *Prog. Energy Combust. Sci.* **2012**, *38*, 215–282. [CrossRef]
17. Hatanaka, T.; Yoda, Y. Attrition of ilmenite ore during consecutive redox cycles in chemical looping combustion. *Powder Technol.* **2019**, *356*, 974–979. [CrossRef]
18. Mendiara, T.; Gayán, P.; Abad, A.; García-Labiano, F.; de Diego, L.F.; Adánez, J. Characterization for disposal of Fe-based oxygen carriers from a CLC unit burning coal. *Fuel Process. Technol.* **2015**, *138*, 750–757. [CrossRef]
19. Ohlemüller, P.; Reitz, M.; Ströhle, J.; Epple, B. Investigation of chemical looping combustion of natural gas at 1 MWth scale. *Proc. Combust. Inst.* **2019**, *37*, 4353–4360. [CrossRef]
20. de Souza-Santos, M.L. A new version of CSFB, comprehensive simulator for fluidised bed equipment. *Fuel* **2007**, *86*, 1684–1709. [CrossRef]
21. de Souza-Santos, M.L. Very high-pressure fuel-slurry integrated gasifier/gas turbine (FSIG/GT) power generation applied to biomass. *Energy Fuels* **2015**, *29*, 8066–8073. [CrossRef]
22. de Souza-Santos, M.L. Proposals for power generation based on processes consuming biomass-glycerol slurries. *Energy* **2017**, *120*, 959–974. [CrossRef]
23. de Souza-Santos, M.L.; Chavez, J.V. Preliminary studies on advanced power generation based on combined cycle using a single high-pressure fluidized bed boiler and consuming sugar-cane bagasse. *Fuel* **2012**, *95*, 221–225. [CrossRef]
24. Moutsoglou, A. A comparison of prairie cordgrass and switchgrass as a biomass for syngas production. *Fuel* **2012**, *95*, 573–577. [CrossRef]
25. de Souza-Santos, M.L.; Chávez, J.V. Development of studies on advanced power generation based on combined cycle using a single high-pressure fluidized bed boiler and consuming sugar cane bagasse. *Energy Fuels* **2012**, *26*, 1952–1963. [CrossRef]
26. Krzywanski, J.; Żyłka, A.; Czakiert, T.; Kulicki, K.; Jankowska, S.; Nowak, W. A 1.5D model of a complex geometry laboratory scale fuidized bed clc equipment. *Powder Technol.* **2017**, *316*, 592–598. [CrossRef]
27. Żyłka, A.; Krzywanski, J.; Czakiert, T.; Idziak, K.; Sosnowski, M.; Grabowska, K.; Nowak, W. Symulacje numeryczne spalania biomasy w pętli chemicznej. *Rynek Energii* **2017**, *133*, 65–72.
28. Zylka, A.; Krzywanski, J.; Czakiert, T.; Idziak, K.; Kulicki, K.; Jankowska, S.; Nowak, W. Numerical simulations of fluidization dynamics in a hot model of a CLC process. *E3S Web Conf.* **2017**, *13*, 04002. [CrossRef]
29. De Souza-Santos, M.L. *Solid Fuels Combustion and Gasification: Modeling, Simulation, and Equipment Operations*, 2nd ed.; CRC Press: Boca Raton, FL, USA, 2010; ISBN 978-1-4200-4749-3.
30. Kunii, D.; Levenspiel, O. *Fluidization Engineering*, 2nd ed.; Elsevier: Oxford, UK, 2013; ISBN 0-409-90233-0.
31. Lucia, U.; Simonetti, M.; Chiesa, G.; Grisolia, G. Ground-source pump system for heating and cooling: Review and thermodynamic approach. *Renew. Sustain. Energy Rev.* **2017**, *70*, 867–874. [CrossRef]
32. Lucia, U.; Grisolia, G. Exergy inefficiency: An indicator for sustainable development analysis. *Energy Rep.* **2019**, *5*, 62–69. [CrossRef]

33. Lucia, U.; Grisolia, G. Cyanobacteria and microalgae: Thermoeconomic considerations in biofuel production. *Energies* **2018**, *11*, 156. [CrossRef]
34. Lucia, U.; Grisolia, G. Unavailability percentage as energy planning and economic choice parameter. *Renew. Sustain. Energy Rev.* **2017**, *75*, 197–204. [CrossRef]
35. Lucia, U.; Fino, D.; Grisolia, G. Thermoeconomic analysis of Earth system in relation to sustainability: A thermodynamic analysis of weather changes due to anthropic activities. *J. Therm. Anal. Calorim.* **2020**. [CrossRef]